CHEMMEDCHEM

CHEMISTRY ENABLING DRUG DISCOVERY

Accepted Article

Title: Total Synthesis of the Endocannabinoid Uptake Inhibitor Guineensine and SAR Studies

Authors: Karl-Heinz Altmann, Ruben Bartholomäus, Simon Nicolussi, Mark Rau, Ana Catarina Simao, Alice Baumann, and Jürg Gertsch

To be cited as: *ChemMedChem* 10.1002/cmdc.201900390

Link to VoR: http://dx.doi.org/10.1002/cmdc.201900390

A Journal of

ChemPubSoc Europe

WILEY-VCH

www.chemmedchem.org

WILEY-VCH

FULL PAPER

Total Synthesis of the Endocannabinoid Uptake Inhibitor Guineensine and SAR Studies

Ruben Bartholomäus,[a] Simon Nicolussi,[b] Alice Baumann,[a] Mark Rau,[b] Ana Catarina Simão,[a] Jürg Gertsch,[b] and Karl-Heinz Altmann*[a]

[a] Dr. R. Bartholomäus (ORCID ID 0000-0003-1696-5045), Msc. ETH A. Baumann, Dr. A. C. Simão, Prof. Dr. K.-H. Altmann (ORCID ID 0000-0002-0747-9734)
Department of Chemistry and Applied Biosciences
ETH Zürich
HCI H405
Vladimir-Prelog-Weg 4
CH-8093 Zürich, Switzerland
E-mail: karl-heinz.altmann@pharma.ethz.ch

[b] Dr. S. Nicolussi (ORCID ID 0000-0003-1260-3282), MSc. M. Rau, Prof. Dr. Jürg Gertsch (ORCID ID 0000-0003-0978-1555)
Institute of Biochemistry and Molecular Medicine
University of Bern, Switzerland
Bühlstrasse 28
CH-3012 Bern, Switzerland

Supporting information for this article is given via a link at the end of the document.

Abstract: Guineensine ((2*E*,4*E*,12*E*)-13-(benzo[*d*][1,3]dioxol-5-yl)-*N*-isobutyltrideca-2,4,12-trienamide) is a plant-derived natural product that inhibits the reuptake of the endocannabinoid anandamide with sub-μM potency. We have established a highly efficient total synthesis of guineensine, which provided the natural product in only 5 steps from commercially available 3-nonyn-1-ol in 17% overall yield, relying on the attachment of the benzodioxolyl moiety to the unsaturated fatty acid chain by means of a Suzuki coupling as the key step. Subsequent SAR studies revealed that the replacement of the *N*-*iso*-butyl group in the natural product by different alkyl, arylalkyl, or aryl groups is generally well tolerated and derivatives could be identified that are slightly more potent anandamide reuptake inhibitors than guineensine itself. In contrast, modifications of the benzodioxolyl moiety led to reduced activity. Intriguingly, a change in the configuration of the C4-C5 double bond from *E* to *Z* was found to be very well tolerated, in spite of the associated change in the overall geometry of the molecule.

Introduction

Guineensine (**1**) (Fig. 1) is an unsaturated fatty acid-derived natural product that belongs to the family of piperamides and was first isolated in 1974 by Okogun et al. from the fruits of *Piper guineense* collected in the western part of Nigeria.[1] Additional members of this natural product family include, e. g., retrofractamides A[2] and B (also known as pipercide),[3] brachystamide B,[4] or laetispicine.[5]

Piperamides have been reported to exhibit a broad range of biological activities, including antibacterial, antitumor, anti-inflammatory, antidiabetic, and antidepressive activities as well as pesticidal effects.[6] Most recently, guineensine (**1**) has attracted significant attention because of its potent and selective inhibition of endocannabinoid (EC) cellular uptake.[7a] Thus, guineensine (**1**) strongly reduces the cellular reuptake of the main endocannabinoid anandamide (AEA) in U937 cells (EC_{50} = 290 nM), while neither inhibiting the EC-degrading enzymes fatty acid amide hydrolase (FAAH) or monoacylglycerol lipase (MAGL) nor interacting with the cannabinoid receptors CB_1 or CB_2 to any significant extent. In vivo, guineensine (**1**) dose-dependently induced cannabimimetic effects in mice, such as strong catalepsy, hypothermia, reduced locomotion and analgesia;[7a] in addition, it was also shown to exhibit pronounced anti-inflammatory effects.[7b] Guineensine (1) is a more potent inhibitor of endocannabinoid uptake than either retrofractamides A/B or brachystamide B, thus highlighting the importance of the length of the connecting chain between the terminal amide group (designated here as the head group) and the benzodioxolyl moiety (tail group) for the inhibition of endocannabinoid uptake.[7a]

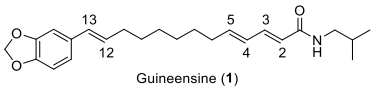

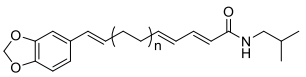

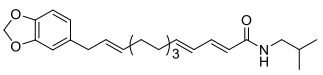

While both the physiological role of FAAH in EC metabolism and the pharmacology of FAAH inhibitors have been well studied,[8] the exact mechanism of EC membrane transport and the pharmacological consequences of the direct, specific inhibition of this process are much less well understood. In particular, it is still unclear if EC membrane transport is mediated by a dedicated membrane transport mechanism[9]. Given its ability to inhibit EC cellular uptake in a potent and selective fashion, the guineensine scaffold represents an attractive structural platform for the development of tool compounds for mechanistic studies, including compounds that would allow to selectively target EC membrane transport. At the same time, guineensine analogs with further improved potency and selectivity could be potential drug

candidates for the treatment of anxiety, pain, chronic stress, or a number of other disorders.[10] The only other potent and *selective* inhibitor of EC reuptake reported to date is (2*E*,4*E*)-*N*-[2-(3,4-dimethoxyphenyl)ethyl]dodeca-2,4-dienamide (WOBE437) that we recently characterized in detail in vitro and in vivo.[11]

To date, three total syntheses of guineensine (**1**) have been reported in the literature. Thus, Okwute et al.[12] described a 9-step synthesis of **1** from catechol already in 1979, but the compound was obtained only in 0.34% overall yield (1.47% from 1,2-(methylenedioxy)benzene). A more efficient approach was subsequently developed by Vig et al.,[13] who were able to access the acid precursor of **1** in 7 steps and ca. 7% overall yield from 1,8-octandiol (no yield was reported for the amide bond-forming step). In the most recent synthesis of **1**, Shingala at al. employed a Julia-Kocienski olefination to establish the C12-C13 double bond, while the dienoate moiety was constructed *via* a Corey-Fuchs alkynylation/Rychnovsky-Trost isomerization sequence. Shingala's synthesis comprised a total of 12 steps from commercial starting materials and gave **1** in 27% overall yield.[14]

No structure-activity relationship (SAR) studies on the effects of guineensine analogs on EC membrane transport have been reported so far, with the exception of a small series of naturally occurring piperamides, including retrofractamides A/B and brachystamide B.[7a] All of these compounds were found to be less potent inhibitors of anandamide cellular uptake than **1**.[7a]

We were interested in the total synthesis of guineensine (**1**) in the broader context of a project aiming (i) at the development of tools that would enable us to target and probe EC cellular transport and (ii) at the identification of highly potent and selective inhibitors of EC transport as leads for drug discovery. To provide a chemical basis for these efforts, we required an effective, concise, and also modular synthesis of **1**, in order to allow diversification of the scaffold both at the arene moiety as well as the amide part. In this report we now disclose a new, efficient total synthesis of guineensine (**1**). The chemistry developed as part of the total synthesis work was subsequently applied to the synthesis of analogs for SAR studies, which have provided first insights into the effect of modifications at either end of the guineensine scaffold on the inhibitory activity for EC membrane transport.

Results and Discussion

Our initial approach towards the synthesis of **1** was to be based on the construction of the C12-C13 *E*-double bond by Julia-Kocienski olefination between sulfone **2** and aldehyde **3** (Scheme 1), in analogy to work reported previously by Shingala et al.[14]

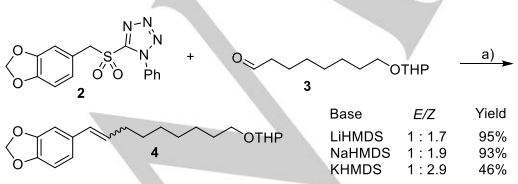

Scheme 1. a) 1. Sulfone **2**, base, THF, -78 °C, 15 min; 2. **3**, THF, -78 °C, 30 min.

Unfortunately, while treatment of **2** with LiHMDS followed by reaction with aldehyde **3** gave the olefin in excellent yield (95% of the mixture of *E*/*Z* isomers), the *E*/*Z* selectivity of the reaction was poor. In fact, the major product of the reaction was the undesired *Z* olefin, which proved to be inseparable from the desired *E* isomer. Subsequent experiments with NaHDMS or KHMDS produced **4** in an even more unfavorable *E*/*Z* ratio (Scheme 1). These findings are in contrast to the results reported by Shingala et al.[14] for the reaction of **2** with the bis-homo (C_{10}) analog of aldehyde **3**. It appears, however, that the reaction in Shingala's case was performed under Barbier conditions, which might affect its stereochemical outcome. (Ref.[14] does not include any experimental protocols). In agreement with our observations, the predominant formation of the *Z* isomer has also been observed in the KHMDS-mediated reaction between 5-(benzylsulfonyl)-1-phenyl-1*H*-tetrazole and decanal in DME.[15] In light of these findings, the Julia-Kocienski approach towards construction of the C12-C13 double bond was abandoned.

Instead, we turned our attention to the use of a Suzuki cross-coupling reaction for the construction of the terminal styryl moiety in **1** (Fig. 1). Given the commercial availability of a broad range of boronic acids, this approach would also enable late stage diversification of the aromatic tail end moiety of the guineensine scaffold as an attractive feature.

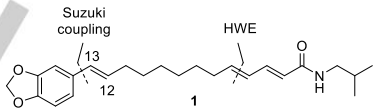

Figure 1. Key retrosynthetic disconnections for the 2nd generation approach towards **1**.

As outlined in Scheme 2, our second generation approach towards **1** departed from (commercially available) 3-nonyn-1-ol (**5**), which was first subjected to an alkyne zipper reaction[16] to shift the triple bond to the terminal position. This was followed by Swern oxidation and subsequent Horner-Wadsworth-Emmons olefination of the ensuing aldehyde with phosphonate **6**, to produce dienoate **7** in 45% overall yield (for the three-step sequence from **5**) and with high stereoselectivity ($\Delta^{4,5}$-*E*/*Z* = 10:1, (*E*/*Z*-$\Delta^{2,3}$ > 20:1). Ester saponification and subsequent amide bond formation *via* the acid chloride proceeded smoothly. The remaining undesired *Z*-$\Delta^{4,5}$ isomer could be removed at this stage by flash chromatography, thus providing dienamide **8** as a single isomer in 84% overall yield from ester **7**. Pd-catalyzed hydrostannylation of the terminal alkyne moiety followed by in situ treatment of the resulting stannane with iodine then gave vinyl iodide **9** in 64% yield. However, this material was only ca. 90% pure; isolation of the intermediate stannane prior to tin-iodide exchange did not yield material of higher purity.[17]

The crucial Suzuki cross-coupling of **9** with boronic acid **10** was initially performed with $Pd(PPh_3)_4$ and Na_2CO_3 in DME/H_2O 3:1, but these conditions gave guineensine (**1**) in only 20% yield with an unsatisfactory purity of 70% (after flash chromatography). Both the yield and purity of the coupling product could be significantly improved by the use of thallium ethoxide[18,19] as an additive, which also reduced the reaction time to 5-10 min. The TlOEt-mediated coupling reaction gave guineensine (**1**) in 34% yield as a ca. 9:1 mixture with what we assume to be the geminally substituted olefin as a side product; the latter could not be removed by conventional flash chromatography. Purification of this mixture was possible by preparative RP-HPLC, to provide

pure guineensine (**1**), whose analytical data were in full agreement with those reported in the literature.[1,12b,20]

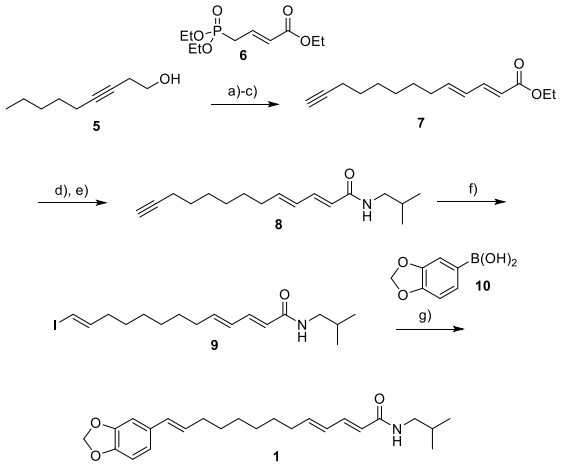

Scheme 2. a) NaH, 1,3-diaminopropane, 70 °C, 80%; b) $(COCl)_2$, DMSO, Et_3N, CH_2Cl_2, -78 °C to rt, 88%; c) **6**, LDA, THF, -78 °C to -20 °C, 64%, $\Delta^{4,5}$-*E*/*Z* = 10:1, $\Delta^{2,3}$-*E*/*Z* > 20:1; d) 2M NaOH, MeOH, 65 °C, quant; e) 1. $(COCl)_2$, CH_2Cl_2, then *iso*-butylamine, Et_3N, 84%; f) 1. Bu_3SnH, $Pd_2(dba)_3$, Cy_3PHBF_4, DIEA, CH_2Cl_2, 0 °C; 2. I_2, CH_2Cl_2, rt, 64%; g) **10**, TlOEt, $Pd(PPh_3)_4$, THF/H_2O 3:1, rt, 34%, $\Delta^{4,5}$-*E*/*Z* > 20:1, $\Delta^{2,3}$-*E*/*Z* > 20:1.

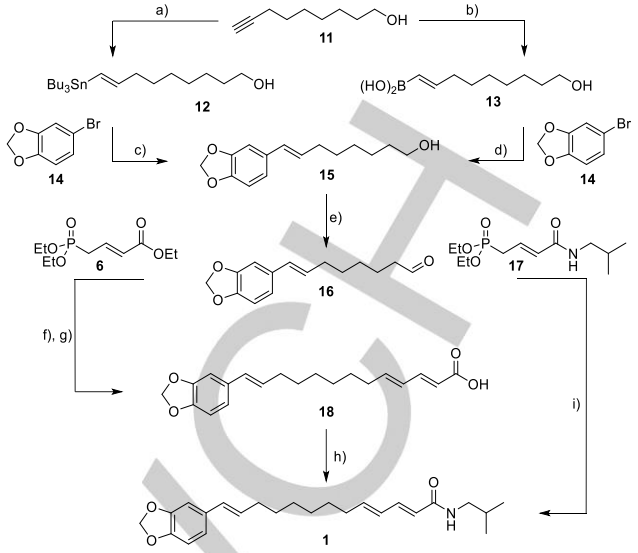

Scheme 3. a) Bu_3SnH, $Pd_2(dba)_3$, Cy_3PHBF_4, DIEA, CH_2Cl_2, 0 °C, 98%; b) catecholborane, THF, 70 °C, then H_2O, rt, 60%; c) $Pd(PPh_3)_4$, DMF, 75 °C, 5 h, 46%; d) $Pd(PPh_3)_4$, Na_2CO_3, DME/H_2O 3:1, 80 °C, 74%; e) $(COCl)_2$, DMSO, Et_3N, CH_2Cl_2, -78 °C to rt, 88%; f) LDA, THF, -78 °C to -20 °C, 68%, $\Delta^{4,5}$-*E*/*Z* = 10:1, $\Delta^{2,3}$-*E*/*Z* >20:1; g) 2M NaOH, MeOH, 60 °C, 99%; h) $(COCl)_2$, then *iso*-butylamine, Et_3N, CH_2Cl_2, 86%; i) LDA, THF, -78 °C to rt, 55%, $\Delta^{4,5}$-*E*/*Z* = 8:1, $\Delta^{2,3}$-*E*/*Z* > 20:1.

While HPLC purification of compounds for biological testing after the final synthetic step is fully acceptable in the context of SAR studies, from a total synthesis perspective, the incomplete selectivity in the transformation of alkyne **8** into vinyl iodide **9** and the resulting formation of an inseparable side product in the subsequent Suzuki coupling step were still unsatisfactory. We thus evaluated an alternative cross-coupling-based strategy towards **1** that involved the early installation of the benzodioxole moiety through Suzuki or Stille coupling between stannane **12** or boronic acid **13**, respectively, and bromide **14** (Scheme 3).

Stannane **12** and boronic acid **13** were both obtained from 8-nonyn-1-ol (**11**) (prepared in one step from **5**; Scheme 2) by palladium-catalyzed hydrostannylation and hydroboration, respectively. Both compounds were obtained as single regio- and stereoisomers after flash column chromatography. While stannane **12** was obtained from **11** in higher yield than boronic acid **13**, the Suzuki coupling of the latter with bromide **14** was more efficient than Stille coupling of the former.[21] Thus, the overall yield for the transformation of **11** into **15** was comparable for both routes (44% vs. 43%). Alcohol **15** was then elaborated into guineensine (**1**) by Swern oxidation, to provide aldehyde **16**, followed by HWE-olefination with phosphonate **6** (which proceeded with excellent stereoselectivity ($\Delta^{4,5}$-*E*/*Z* = 10:1, $\Delta^{2,3}$-*E*/*Z* > 20:1)), ester saponification and finally amide bond formation via the acid chloride. The undesired, minor $\Delta^{4,5}$-*Z* isomer originating from the HWE reaction could be removed after the coupling step by flash column chromatography, to give guineensine (**1**) as a single isomer in a total yield of 18% for the seven-step sequence from **5** (as the ultimate commercial starting material). The number of linear steps could be further reduced by directly reacting aldehyde **16** with phosphonate **17** (for the preparation of **17** see the SI). This highly convergent approach provided guineensine (**1**) in a total yield of 17% for a longest linear sequence of five steps (from **5**). This represents the shortest and most efficient synthesis of this natural product reported to date.

With an efficient total synthesis of the natural product established, we turned our attention to the synthesis of selected analogs, in order to gain first insights into the SAR of **1** with regard to inhibition of EC transport. As illustrated in Scheme 4, we have utilized acid **18** to prepare head-group modified variants of guineensine with variations in the size, lipophilicity and aliphatic/aromatic character of the amide moiety. In all cases, the coupling reaction via the in situ generated acid chloride proceeded smoothly and provided the desired products **19** in yields between 59% and 86% after purification by flash column chromatography. For most of the analogs **19**, the $\Delta^{4,5}$-*Z* isomer originating from the imperfect stereoselectivity of the HWE olefination between **16** and **6** could be removed after the coupling reaction. In all other cases the fraction of $\Delta^{4,5}$-*Z* isomer in the final product was lower than 10%.

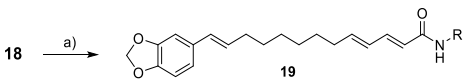

Scheme 4. a) 1. $(COCl)_2$, CH_2Cl_2, rt, 30 min. 2. R-NH_2, Et_3N, CH_2Cl_2, rt, 15 min, 59-86%. For the structure of substituents R see Table 1.

The preparation of guineensine analogs with modifications of the aryl moiety was based on vinyl iodide **9** (10:1 mixture of isomers, *vide supra*), which was converted into structures **20** by means of Suzuki coupling with a series of boronic acids under the conditions elaborated for the synthesis of the natural product. (Scheme 5).

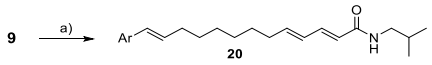

Scheme 5. a) Ar-B(OH)$_2$, TlOEt, Pd(PPh$_3$)$_4$, THF/H$_2$O 3:1, rt, 37-52% (ca. 90% purity). For the structures of Ar see Table 2.

As for the synthesis of **1**, analogs **20** were generally contaminated with ca. 10% of a side product that could not be removed by flash column chromatography; however, all products **20** could be obtained in analytically pure form by final RP-HPLC purification.
In addition to the assessment of head and tail group modifications, we have also investigated analogs **21** and **22**, which are characterized by a higher and lower level of saturation of the C12-C13 bond, respectively, and we have determined the importance of the configuration of the C4-C5 double (analog **23**).

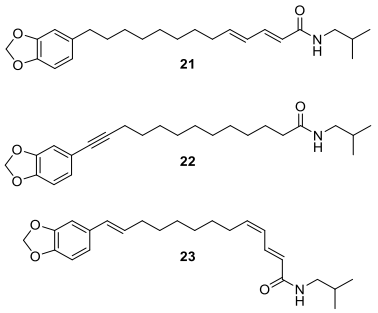

As illustrated in Scheme 6, analog **21** was elaborated from THP-ether **4** (mixture of double bond isomers; Scheme 1), which was converted into aldehyde **24** by THP-ether cleavage, followed by catalytic hydrogenation and subsequent DMP oxidation in 80% overall yield. Aldehyde **24** was then elaborated into **21** in analogy to the preparation of guineensine (**1**) from **16** (cf. Scheme 3).

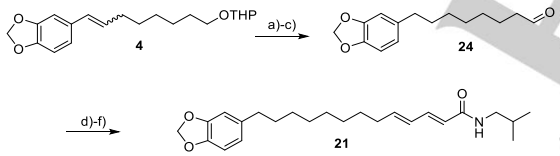

Scheme 6. a) TsOH, MeOH, 95%; b) H$_2$, Pd/C, EtOH, 95%; c) (COCl)$_2$, DMSO, Et$_3$N, CH$_2$Cl$_2$, -78 °C to rt, 84%; d) **6**, LDA, THF, -78 °C to -20 °C, 70%, $\Delta^{4,5}$-*E*/*Z* = 10:1; e) 2M NaOH, MeOH, 70 °C, 76%; f) EDC, HOBt, Et$_3$N, *iso*-butylamine, CH$_2$Cl$_2$, 59%.

Analog **22** was obtained from alkyne **8** (Scheme 2) and bromide **14** (Scheme 3) by Sonogashira coupling (Scheme 7), while **23** was isolated as a minor side product from the reaction of acid **18** (as a ca. 10:1 mixture of $\Delta^{4,5}$-*E*/*Z* isomers) with *iso*-butyl amine (*vide supra*).

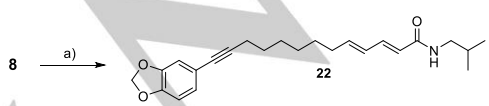

Scheme 7. a) **14**, Pd(PPh$_3$)$_2$Cl$_2$, CuI, *n*-BuNH$_2$, 60 °C, 30 min, 11%.

All compounds were assessed for their ability to inhibit AEA transport into U937 cells, using radiolabeled AEA as the transport substrate.[7a] As AEA uptake is also reduced upon inhibition of FAAH, the inhibitory activity of guineensine analogs against FAAH was also determined independently.[7a] The corresponding data are summarized in Tables 1 and 2 for head group (cpds. **19**) and tail group (cpds. **20**) modifications, respectively.

Table 1. Inhibition of AEA uptake into U937 cells by head group-modified guineensine analogs **19**.

Cpd.[a]	R[a]	EC$_{50}$ [μM] (95% CI)[b]	Maximum inhibition (%)[c]	% FAAH inhibition at 1 μM[d]
1		0.288 (0.190-0.437)	>60	44.1[e]
19a	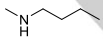	0.409 (0.267-0.626)	>60	0
19b		0.374 (0.268-0.523)	>60	0
19c		0.596 (0.394-0.900)	>60	37
19d		0.661 (0.345-1.266)	>60	12
19e		1.50 (0.911-5.028)	>60	14[f]
19f		0.972 (0.286-1.613)	>60	3[f]
19g		0.438 (0.252-0.764)	>60	23[f]
19h	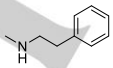	0.344 (0.201-0.590)	>60	22
19i	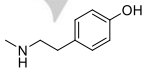	0.123 (0.095-0.158)	>60	30
19j	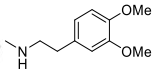	0.097 (0.062-0.218)	>60	7
19k	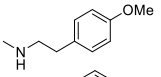	>10	45	0[f]
19l	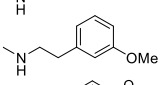	0.096 (0.071-0.130)	>60	42
19m	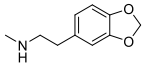	0.112 (0.074-0.169)	>60	35
19n	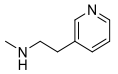	0.463 (0.267-0.801)	>60	17
19o		0.81 (0.058-0.112)	>60	2
19p	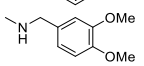	0.116 (0.062-0.218)	>60	7
19q		0.232 (0.145-0.370)	>60	8
19r	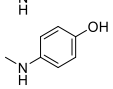	1.70 (1.04-2.80)	ND[g]	0[f]
19s		0.579 (0.337-0.994)	83	0

[a] For the general structure of analogs **19**, *cf*. Scheme 4. [b] Concentration required for half-maximal inhibition of uptake of AEA into U937 cells. EC$_{50}$ values represent the mean of at least three independent experiments. 95% CI, 95% confidence interval. [c] Maximal inhibition of uptake of AEA into U937 cells. Maximum inhibition data in our uptake assay data varied significantly; thus, at this point, we consider numbers >60% as essentially indistinguishable. [d] Inhibition of FAAH in U937 cell homogenates. In general, 1 μM was the highest concentration tested. [e] IC$_{50}$ value. [f] IC$_{50}$ >10 μM. [g] ND, not determined.

With one single exception, none of the head group modifications investigated here, which include the replacement of the natural *N*-*iso*-butyl group by other alkyl groups as well as differently substituted arylalkyl and aryl moieties, led to a substantial decrease in AEA uptake inhibition (Table 1). In fact, 16 out of 19 different analogs exhibited sub-μM EC_{50} values, with even compounds **19e** and **19r** still being active in the low single digit μM range. Interestingly, while *N*-methyl amide **19e** is less active than all other *N*-alkyl amides, a re-increase in potency is observed for the less hydrophobic primary amide **19g**; the latter is not significantly less active than guineensine (**1**). As has been reported for guineensine (**1**), none of the compounds is able to block AEA uptake completely, which is in line with previous findings on other types of AEA uptake inhibitors. The possible reasons for this observations have been discussed[7a] and the arguments shall not be repeated here. Importantly, none of the analogs showed effects on FAAH activity that would suggest a major contribution of FAAH inhibition to the reduction in AEA uptake, certainly not for those analogs with activity similar to or better than that of guineensine (**1**). Five compounds (**19i**, **j**, **l**, **m**, **p**) appear to be between 2- and 3-fold more potent than **1**, although the 95% confidence interval in all cases overlaps with that of **1** and the differences, thus, should not be overinterpreted. It should be noted, however, that the most potent compound identified here (**19j**) incorporates a (3,4-dimethoxyphenyl)ethyl substituent on the amide nitrogen. The same amide head group is also part of the recently described potent and selective AEA uptake inhibitor (2*E*,4*E*)-*N*-(3,4-dimethoxyphenethyl)dodeca-2,4-dienamide (WOBE437)[11] and thus seems to be a privileged structural feature for fatty acid amide-based AEA cellular uptake inhibitors. Noteworthy, the *ortho*-dimethoxyphenyl motif is also found in benzylamide **19p**; the inhibitory activities of *N*-(3,4-dimethoxyphenyl)ethyl amide **19j** and of *N*-3,4-dimethoxybenzyl amide **19p** are 3-fold and 6-fold higher, respectively, than for the corresponding unsubstituted parent compounds **19i** and **19o**.

As the sole example within the series of head group-modified guineensine analogs investigated, compound **19k** is dramatically less potent than the natural product. In light of the sub-μM activity of analogs **19i** and **19j**, the loss in potency incurred by **19k** is unexpected and may in fact raise questions about the validity of the result. However, the poor activity of **19k** was reproduced with two different batches of material (i. e. originating from two separate synthesis campaigns) and we are confident about the reliability of the data also for this analog.

In contrast to head group-modified guineensine analogs **19**, all of the investigated tail group-modified variants **20** exhibit reduced activity compared to **1** (Table 2). Strikingly, a dramatic drop in AEA uptake inhibition is observed for analogs **20b** and **20f**, both of which incorporate a methoxy group in the *para* position of the terminal styryl moiety. This finding suggests that substitution at this position is not tolerated outside of the context of the bicyclic benzo[*d*][1,3]dioxole (or perhaps a closely related bicyclic) moiety that is present in the natural product, although this may also depend on the exact nature of the substituent. We note, however, that we cannot rule out the possibility that **20b** and **20f** exhibit particularly low solubility, which would obscure the results. Interestingly, the replacement of the benzo[*d*][1,3]dioxolyl group by an indole moiety (analog **20h**) produces a reasonably potent FAAH inhibitor and the inhibition of AEA uptake by this compound may largely be attributed to its FAAH inhibitory activity. Finally, and perhaps not too surprisingly, the complete removal of the benzo[*d*][1,3]dioxole moiety from guineensine (**1**) leads to a sharp drop in activity, although not to the same extent as for analogs **20b** and **20f**.

Table 2. Inhibition of AEA uptake into U937 cells by tail group-modified guineensine analogs **20**.

Cpd.[a]	R[a]	EC_{50} [μM] (95% CI)[b]	Maximum inhibition (%)[c]	% FAAH inhibition at 10 μM[d]
20a		3.59 (1.00-12.86)	>60	24
20b	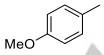	>100	41	29[e]
20c	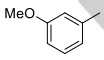	1.3 (0.9-1.9)	>60	35
20d		11.0 (12.0-6.1)	>60	33
20e	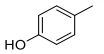	6.0 (3.6-10.1)	60	21[f]
20f	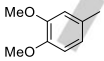	>100	32	12[g]
20g	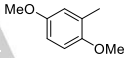	0.849	50	31[g]
20h		1.66 (1.16-2.36)	>60	2.4[h]
8	-	5.75 (4.33-7.63)	>60	11

[a] For the general structure of analogs **19**, *cf*. Scheme 4. [b] Concentration required for half-maximal inhibition of uptake of AEA into U937 cells. EC_{50} values represent the mean of at least three independent experiments. 95% CI, 95% confidence interval. [c] Maximal inhibition of uptake of AEA into U937 cells. Maximum inhibition data in our uptake assay data varied significantly; thus, at this point, we consider numbers >60% as essentially indistinguishable. [d] Inhibition of FAAH in U937 cell homogenates at 10 μM compound concentration. [e] 100 μM. [f] 5 μM. [g] 1 μM. [h] IC_{50} value [μM].

A very moderate loss in activity is also observed upon formal reduction of the C12-C13 double bond in guineensine (**1**) (ca. 2-fold, Table 3).

Table 3. Inhibition of AEA uptake into U937 cells by backbone-modified guineensine analogs **21**-**23**.

Cpd.[a]	EC_{50} [μM] (95% CI)[b]	Maximum inhibition (%)[c]	% FAAH inhibition at 1 μM[d]
21	0.533 (0.317-0.895)	>60	7
22	1.16 (0.70-1.92)	>60	0
23	0.134 (0.047-0.384)	47	0

[a] For the structure of analogs **21**-**23** see text. [b] Concentration required for half-maximal inhibition of uptake of AEA into U937 cells. EC_{50} values represent the mean of at least three independent experiments. 95% CI, 95% confidence interval. [c] Maximal inhibition of uptake of AEA into U937 cells. Maximum inhibition data in our uptake assay data varied significantly; thus, at this point, we consider numbers >60% as essentially indistinguishable. [d] Inhibition of FAAH in U937 cell homogenates at 1 μM compound concentration.

A somewhat more pronounced effect (ca. 4-fold reduction in potency compared to **1**) is associated with the replacement of the C12-C13 double bond by a triple bond, although this modification leads to a distinct change in the orientation of the aromatic tail group relative to the alkyl chain. Intriguingly, the change in the configuration of the C4-C5 double bond from *E* to *Z* does not affect potency, in spite of the significantly different overall shape of the corresponding analog **23**. However, compared to **1**, the maximum efficacy observed for analog **23** is lower; although the significance of this observation is not clear at this point.

Conclusions

We have established a new and highly efficient total synthesis of the natural endocannabinoid reuptake inhibitor guineensine (**1**), which provides the natural product in 5 steps (longest linear sequence) and 17% overall yield. The chemistry developed in the course of the total synthesis work was then exploited for the synthesis of a series of analogs, which have offered first insights into the SAR of guineensine-derived AEA uptake inhibitors. Thus, the natural *N*-*iso*-butyl substituent on the terminal amide group can be replaced by a number of alkyl, arylalkyl, or aryl groups without a significant decrease in potency; some analogs are even slightly more potent than **1**. At first glance, the inhibition of AEA uptake appears to track with the hydrophobicity of the group attached to the amide nitrogen. However, as illustrated by the excellent activity of primary amide **19g** and the poor activity of **19k**, the situation must be more complex, even if our findings cannot be rationalized at this point. Compared to the amide moiety, the benzo[*d*][1,3]dioxole tail group appears to be more sensitive to structural changes and all of the analogs **20** were found to be less potent than **1**. While we have only studied a very limited number of tail group-modified guineensine variants at this point, the data again suggest that AEA cellular uptake inhibition, as for the amide moiety, is not simply related to the presence of a (any) hydrophobic tail group, but clearly depends on the exact structure of this group. In line with our previous studies[11][22], AEA membrane transport can be potently inhibited independent of FAAH with a distinctive SAR indicative of a protein target. Overall, our work presents the basis for the design and synthesis of more advanced guineensine analogs or, more generally, fatty acid amide-derived AEA cellular uptake inhibitors, with the ultimate goal of developing more drug-like structures. Work along these lines in combination with efforts aiming at the identification of the target of EC membrane transport inhibitors are currently ongoing in our laboratories.

Experimental Section

Detailed protocols for the synthesis of all final products and intermediates, analytical data for all new compounds, and copies of the relevant ^{1}H- and ^{13}C-NMR spectra can be found in the SI.

Acknowledgements

This research was supported by the Swiss National Science Foundation through the National Centre of Competence in Research (NCCR) TransCure. We are indebted to Dr. Bernhard Pfeiffer and Leo Betschart for NMR support, to Dr. Xiangyang Zhang, Louis Bertschi, Rolf Häfliger, and Oswald Greter for HRMS spectra, and to Kurt Hauenstein for general technical support. We thank Patricia Schenker und Tatiana Hofer for excellent support with compound testing.

Conflict of interest

This authors declare no conflict of interest.

Keywords: endocannabinoids • endocannabinoid mebrane transport • guineensine • natural product • total synthesis

References:

[1] J. I. Okogun, D. E. U. Ekong, *J. Chem. Soc. Perkin Trans. 1* **1974**, 1-4.
[2] A. Banerji, D. Bandyopadhyay, M. Sarkar, A. K. Siddhanta, S. C. Pal, S. Ghosh, K. Abraham, J. N. Shoolery, *Phytochemistry* **1985**, *24*, 279-284.
[3]` M. Miyakado, I. Nakayama, H. Yoshioka, N. Nakatani, *Agricult. Biol. Chem.* **1979**, *43*, 1609-1611.
[4] A. Banerji, C. Das, *Phytochemistry* **1989**, *28*, 3039-3042.
[5] C. Y. Yao, J. Wang, D. Dong, F. G. Qian, J. Xie, S. L., Pan, *Phytomedicine* **2009**, *16*, 823-829.
[6] For recent reviews, cf.: a) S. K. Okwute, H. O. Egharevba, *Int. J. Chem.* **2013**, *5*, 99-122. b) J. C. do Nascimento, V. F. de Paula, J. M. David, J. P. David, *Quim. Nova* **2012**, *35*, 2288-2311.
[7] a) S. Nicolussi, J. M. Viveros-Paredes, M. S. Gachet, M. Rau, M. E. Flores-Soto, M. Blunder, J. Gertsch, *Pharmacol. Res.*, 2014, **80**, 52–65. b) I. Reynoso-Moreno, I. Najar-Guerrero, N. Escareño, M. Eduardo Flores-Soto, J. Gertsch, J. M. Viveros-Paredes, *J. Agric. Food Chem.* **2017**, *65*, 9435-9442.
[8] For recent reviews, see: a) W. Tuo, N. Leleu-Chavain, J. Spencer, S. Sansook, R. Millet, P. Chavatte, Philippe, *J. Med. Chem.* **2017**, *60*, 4-46. b) S. Ogawa, H. Kunugi, *Curr. Neuropharmacol.* **2015**, *13*, 760-775.
[9] a) S. Nicolussi, J. Gertsch, *Vitam. Horm.* **2015**, *98*, 441-485. b) C. J. Fowler, *Trends Pharmacol. Sci.* **2012**, *33*, 181-185. c) R. Mechoulam, D. G. Deutsch, *Proc. Natl. Acad. Sci. USA* **2005**, *102*, 17541–17542.
[10] P. Pacher, *Pharmacol. Rev.* **2006**, *58*, 389-462.
[11] A. Chicca, S. Nicolussi, R. Bartholomäus, M. Blunder,d, A. Aparisi Rey, V. Petruccia, I. del Carmen Reynoso-Moreno, J. M. Viveros-Paredes, M. D. Gensa, B. Lutz, H. B. Schiöth, M. Soeberdt, C. Abels, R.-P. Charles, K.-H. Altmann, J. Gertsch, *Proc. Natl. Acad. Sci. USA* **2017**, *114*, E5006-E5015
[12] a) S. K. Okwute, D. A. Okorie, J. I. Okogun, *Nig. J. Nat. Sci.* ***1979***, *1*, 9-11. The synthesis was later republished with a 1.08% overall yield from 1,2-(methylenedioxy)benzene: b) S. K. Okwute, J. I. Okogun, D. A. Okorie, *Tetrahedron* **1984**, *40*, 2541-2545.
[13] O. P. Vig, S. D. Sharma, O. P. Sood and S. S. Bari, *Indian J. Chem.* **1980**, *19B*, 350-352.
[14] S. D. Shingala, G. V. Reddy, R. S. C. Kumar, P. A. Yadav and K. S. Babu, *J. Asian Nat. Prod. Res.* **2011**, *13*, 128-135.
[15] P. J. Kocienski, A. Bell, P. R. Blakemore, *Synlett* **2000**, 365-366.
[16] C. A. Brown, A. Yarnashita, *J. Am. Chem. Soc.* **1975**, *97*, 891-892.
[17] The generation of a vinyl iodide functionality already at the stage of ester **7** would have provided a valuable substrate for two-site diversification, but was not successful. A complex mixture of products was obtained upon attempted hydrostannylation of **7**, probably caused by reduction of the dienoate moiety by Bu_3SnH.
[18] S. Frank, H. Chen, R. K. Kunz, M. J. Schnaderbeck, W. R. Roush, *Org. Lett.* **2000**, *2*, 2691-2694.
[19] F. Glaus, K.-H. Altmann, *Angew. Chem. Int. Ed.* **2015**, *54*, 1937-1940.
[20] F. Kiuchi, N. Nakamura, Y. Tsuda, K. Kondo, H. Yoshimura, *Chem. Pharm. Bull.* **1988**, *36*, 2452-2465.

[21] Stille coupling between stannane **12** and triflate **24** gave **15** in essentially the same yield as the reaction with bromide **14**.

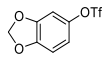

24

[22] S. Nicolussi, A. Chicca, M. Rau, S. Rihs, M. Soeberdt, C. Abels, J. Gertsch, *Biochem. Pharmacol.* **2014**, *92*, 669-689.

[23] M. Rau, S. Nicolussi, A. Chicca, J. Gertsch, *Meth. Mol. Biol.* **2016**, *1412*, 191-203.

WILEY-VCH

FULL PAPER

Entry for the Table of Contents

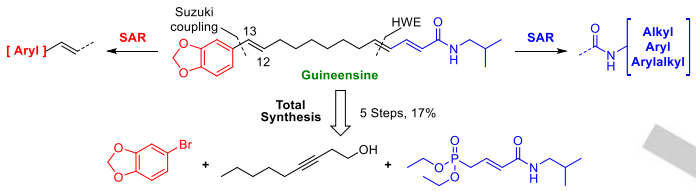

The piperamide guineensine is a potent inhibitor of endocannabinoid uptake. We have developed an efficient and scalable total synthesis of guineensine, which has also served as a platform for the synthesis of analogs with modified end groups. While modifications of the N-substituent on the amide nitrogen were generally well tolerated, the benzodioxolyl group was more sensitive to structural changes. This group may represent a specific structural requirement for inhibition of endocannabinoid uptake by guineensine and other piperamides.